Role of the *iroquois3* homeobox gene in organizer formation

Tetsuhiro Kudoh and Igor B. Dawid†

Laboratory of Molecular Genetics, National Institute of Child Health and Human Development, National Institutes of Health, Bethesda, MD 20892

Contributed by Igor B. Dawid, May 4, 2001

In zebrafish, the organizer is thought to consist of two regions, the yolk syncytial layer (YSL) and the shield. The dorsal YSL appears to send signals that affect formation of the shield in the overlying mesendoderm. We show here that a domain of dorsal deep cells located between the YSL and the shield is marked by expression of the *iro3* gene. As gastrulation proceeds, the *iro3* positive domain involutes and migrates to the animal pole. *Iro3* expression is regulated by Nodal and bone morphogenic protein antagonists. Overexpression of *iro3* induced ectopic expression of shield-specific genes. This effect was mimicked by an Iro3-Engrailed transcriptional repressor domain fusion, whereas an Iro3-VP16 activator domain fusion behaved as a dominant negative or antimorphic form. These results suggest that Iro3 acts as a transcriptional repressor and further implicate the *iro3* gene in regulating organizer formation. We propose that the *iro3*-expressing dorsal deep cells represent a distinct organizer domain that receives signals from the YSL and in turn sends signals to the forming shield, thereby influencing its expansion and differentiation.

In the early vertebrate embryo, specification of the dorso-anterior axis is a critical step in body patterning that is promoted by a small dorsal region called the Spemann organizer. In *Xenopus laevis*, multiple regions are involved in organizer formation and function (1). The Nieuwkoop center, residing in the dorsal endodermal layer at mid to late blastula, has a role in organizer induction, and its formation is initiated by β-catenin signaling (2–4). In the zebrafish embryo, the dorsal yolk syncytial layer (YSL) may be analogous to the Nieuwkoop center (5–7), and its position is marked by the homeobox gene *bozozok (dharma*, *nieuwcoid*) (8–10). The shield, a region of dorsal mesendoderm that mainly gives rise to the prechordal plate and notochord, is the zebrafish equivalent of the Spemann organizer (11, 12).

In this article, we propose an additional organizer subdomain in zebrafish residing at the vegetal side of the shield in dorsal mesendoderm as identified by expression of the homeobox gene *iroquois3* (*iro3*). *Iroquois* genes were discovered in *Drosophila* as neural prepattern genes regulating proneural genes in the *achaete–scute* complex (*as–c*) (13, 14). Loss of *iroquois* genes alters neural differentiation, wing formation, and dorsoventral polarity in the head region (15–19). *Iroquois* genes have recently been isolated from several vertebrates. *Xenopus iro1*, *iro2*, and *iro3* induce proneural markers including the *as–c* homolog *Xash3* (20, 21). In chicken, *irx4* is expressed in heart ventricles and regulates ventricle/atrium cell fate determination (22). Zebrafish *iro3* was reported to be expressed in the notochord in the late gastrula and in the neural tube during somitogenesis (23). Here, we report isolation of an additional *iro3* cDNA, which we demonstrate to be the major splicing variant. We show that *iro3* is also expressed in the dorsal deep layer during blastula and gastrula and that early *iro3* expression is regulated by Nodal and anti-bone morphogenic protein (BMP) signals. We further show that ectopic expression of *iro3* can induce several organizer genes. These results suggest that the *iro3*-expressing region delineates a distinct organizer subdomain and that *iro3* has a role in organizer formation and function.

Materials and Methods

Radiation Hybrid Mapping. *Iro3* was mapped on the LN54 radiation hybrid panel (24), using the primers cattgtaagcatgtcctgtg and ttcggatcacaagtatatac.

Reverse Transcriptase (RT)-PCR of *iro3* Transcripts. Total RNA (2 μg) was reverse-transcribed by Superscript II reverse transcriptase in 20-μl reactions, and 1 μl of this reaction was amplified by PCR using *Taq* polymerase (Roche Molecular Biochemicals) in a 50-μl reaction under the following conditions: 94°C, 1 min; 60°C, 1 min; and 72°C, 2 min for 35 cycles, using primers 1062F/ggcgaaccggtcaaaatcaa, 1459R/gcttccaaggcactagatc, 1439F/gatctagtgccttggaagc, and 1743R/acatcaaatcctcacagagc.

***Iro3*, *En-iro3*, and *VP-iro3* Expression Constructs.** The *Iro3* coding region was amplified by PCR and subcloned into the pCS2 + expression vector. For the construction of *En-iro3*, the *iro3* sequence encoding the homeodomain and flanking region (82–204 aa) was amplified by PCR, using primers ggcgaattcgccgc-catgggcgtccagcatcctggatttg and ggcgaattccgtaaacatttccttcctcgtc. The product was inserted into the *Eco*RI site upstream of the *engrailed* repressor domain in pCS2 + En (25). To generate *VP-iro3*, the same region was amplified by using primers gcctc-gagggcgtccagcatcctggatttgc and gctctagagtaaacatttccttcctcg and inserted into the *Xba*I/*Xho*I sites upstream of the VP16 activator domain in pCS2 + VP16 (25).

mRNA Synthesis and Embryo Injections. mRNA was synthesized by MMESSAGE MMACHINE (Ambion, Austin, TX). The following genes were injected: *iro3*, *En-iro3*, *VP-iro3*, *squint* (*sqt*) and *cyclops* (*cyc*) (26), *TaramA** (27), *β-catenin* (4), and mouse *noggin* (gift of M. Hibi, Osaka University, Osaka).

Whole-Mount *in Situ* Hybridization. Embryos were fixed in 4% paraformaldehyde in PBS at 4°C and manually dechorionated. Embryos were stored in methanol, permeabilized in acetone for 8 min, and rehydrated in 0.1% Tween-20 in PBS. The *in situ* hybridization was performed essentially as described (28). The following probes were used: *iro3*, *ntl*, *gsc*, *sqt*, *cyc*, *axl*, *lim1*, *BMP2b*, *BMP4*, *chd*, *nog1*, *follistatin*, *dkk1*, *sox17*, and *mixer*. β-galactosidase (β-gal) was stained by Salmon-β-D-galactoside (Biosynth, Naperville, IL).

Mutant Analysis. The following mutants were used for *in situ* hybridization: *one eye pinhead*^{m134} (*oep*), *squint*^{cz35} (*sqt*),

Abbreviations: BMP, bone morphogenic protein; YSL, yolk syncytial layer; RT, reverse transcriptase; β-gal, β-galactosidase.

Data deposition: The sequence reported in this paper has been deposited in the GenBank database (accession no. AF340184).

†To whom reprint requests should be addressed. E-mail: idawid@nih.gov.

The publication costs of this article were defrayed in part by page charge payment. This article must therefore be hereby marked "*advertisement*" in accordance with 18 U.S.C. §1734 solely to indicate this fact.

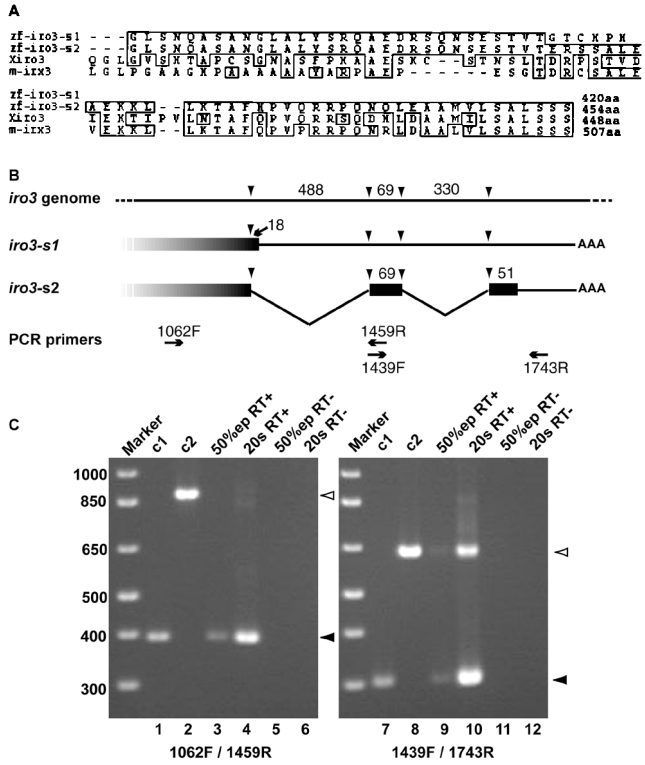

Fig. 1. (*A*) Alignment of C-terminal sequences between zebrafish Iro3 splice variants, *Xenopus* iro3 (Xiro3), and mouse Irx3 (*m*-irx3) proteins. Iro3-s1 is from Tan *et al.* (23); Iro3-s2 is reported in the present work. Iro3-s2 contains 40 aa at the C terminus that are different from Iro3-s1; this region has high homology to Xiro3 and *m*-irx3. (*B*) Structure of *iro3-s1 and iro3-s2* mRNA at the 3′ region compared with *iro3* genomic sequence. In this genomic region, four splice sites (arrowheads) could be identified, defining two introns of 488 and 330 nt in length. Whereas *iro3-s2* is fully spliced, *iro3-s1* is essentially identical to *iro3* genomic DNA in this region. Translation of the penultimate intron in *iro3-s1* leads to the addition of six nonhomologous amino acids and premature termination. Two pairs of RT-PCR primers, designed to detect these two putative introns, are indicated below the maps. (*C*) Ratio of spliced and unspliced mRNA of *iro3.* C1 and C2 represent *iro3-s2* cDNA and *iro3* genomic DNA, respectively, used as control templates. Total RNA was prepared from 50% epibody (50%ep) and 20 somite stages (20s), reverse-transcribed (RT+), and amplified by PCR using the primers indicated. Open arrowhead, unspliced product; closed arrowhead, spliced product.

cyclops^{b16} (*cyc*), *no tail* (*ntl*), *floating head*^{n1} (*flh*), *swirl*^{tc300} (*swr*), and *chordino*^{tt250} (*din*).

Results

Cloning of *iro3* cDNA. We isolated a cDNA for the *iro3* homeobox gene during an *in situ*-based screen (T. K. M. Tsang, N. A. Hukriede, J. Chen, M. Dedekian, C. J. Clarke, A. Kiang, S. Schultz, J. A. Epstein, R. Toyama & I.B.D., unpublished observation). Recently, Tan *et al.* (23) reported the cloning of an *iro3* cDNA. Our *iro3* isolate encodes a different sequence in the C-terminal 40 aa; we refer to the Tan *et al.* clone as *iro3-s1* and to our clone as *iro3-s2*. Iro3-s2 is similar to Xiro3 and mouse Irx3 throughout the C terminus, whereas similarity of Iro3-s1 and the frog and mouse proteins ends abruptly upstream of the C terminus (Fig. 1*A*). *Iro3* genomic DNA was sequenced, proving to be very similar to *iro3-s1* in this region, with only a few differences that may be polymorphisms (not shown), suggesting that *iro3-s1* represents incompletely spliced mRNA that terminates prematurely (Fig. 1*B*).

The ratio of splicing variants of *iro3* was examined by RT-PCR with RNA from 50% epibody and 20 somite embryos. The spliced variant was the major product at both stages, although the unspliced variant, including the last intron, was easily detectable (Fig. 1*C*).

The *iro3* gene was mapped by the radiation hybrid method with the LN54 panel (24). The gene resides on LG7, with the closest marker being Z6819 (see http://mgchd1.nichd.nih.gov:8000/zfrh/current.html for details).

***Iro3* Expression in the Blastula and Gastrula Embryo.** We found expression of the *iro3* gene in a unique pattern in the mesendodermal layer of the early embryo, as illustrated by double-label *in situ* hybridization with the mesodermal marker *no tail* (*ntl*) and the organizer marker *goosecoid* (*gsc*) (Fig. 2). *Iro3* was expressed initially at the sphere stage on one side of the blastoderm margin, expanding throughout the margin by 30% epibody, when *iro3* and *ntl* domains largely coincide. At 40% epibody, *ntl* expands slightly toward the animal pole, whereas *iro3* remains restricted to the vegetal side of the margin (Fig. 2*C*), similar to the pattern of the endodermal marker *gata5* (29) (Fig. 2*V*), and *squint (sqt)* (26) (Fig. 2*W*). The similarity to *gata5* implies that *iro3* expression marks a presumptive endodermal domain. At the 50% epibody stage, when the marginal layer starts to involute, *iro3* expression becomes restricted to the dorsal side. The *iro3* domain involutes toward the animal pole, and at midgastrula a few *iro3*-positive cells surround the anterior edge of the prechordal plate that is marked by *gsc* (Fig. 2 *E* and *O*, arrowhead). *Iro3* RNA disappears from the deep layer around the bud stage (not shown). As previously described, *iro3* is also expressed in the notochord at the late gastrula stage and in the neural tube during somitogenesis (23).

***Iro3* Expression Is Regulated by a Nodal Signal.** In *sqt*$^{-/-}$ embryos, where a *nodal* family gene is defective (30), *iro3* expression was specifically lost on one side of the margin at 40% epibody (Fig. 3*A2*, arrow). This is most likely the dorsal side, as *sqt* embryos at 65% epibody miss *iro3* expression dorsally, whereas some staining remains at the edges of the defective dorsal domain (Fig. 3*A4*, arrow). In *one eye pinhead* (*oep*) mutants where the activity of all Nodal factors is impaired (31), *iro3* expression was lost entirely (Fig. 3*B1*). Other mesendodermal mutants including *cyclops* (*cyc*), *no tail* (*ntl*), and *floating head* (*flh*) did not show obvious defects in *iro3* expression during gastrulation.

We compared the responses of *iro3* and *ntl* to Nodal signaling. Whereas *ntl* was induced by injection of low doses of *sqt* mRNA, *iro3* was only induced at high doses (Fig. 3 *C1*, *C2*, *D1*, and *D2*). Further, *ntl* was induced at a distance from the *sqt* injection domain, which was marked by β-gal, but *iro3* was restricted to the marked region (Fig. 3 *C2* and *D2*). Similar results were obtained by overexpression of the Nodal factor Cyclops, by Activin, and by the activated form of the putative Nodal receptor TaramA* (27) (Fig. 3 *C3* and *D3*; data not shown). When mRNA encoding the Nodal inhibitor Antivin was injected, *iro3* expression was inhibited at a low dose, whereas *ntl* was suppressed only at a higher dose (Fig. 3 *E1–F4*). Thus, *ntl* responds to a low level of Nodal signaling, whereas *iro3* requires a high level for its activation. The difference in levels of Nodal signaling required for induction of *ntl* and *iro3* is consistent with previous reports in *Xenopus* and zebrafish, showing that endoderm induction requires higher levels of Nodal/Activin signaling than mesoderm induction (29, 32–34).

***Iro3* Expression Is Regulated by β-Catenin and BMP Signals.** In *swirl* (*swr*) mutants, which are defective in *bmp2b* (35), the normal dorsally restricted *iro3* expression was expanded ventrally (Fig. 3*B3*). Consistently, injection of RNA encoding the BMP antagonist Noggin induced ventral expansion of *iro3* (Fig. 3*H2*), and hyperdorsalized embryos generated by LiCl treatment expressed *iro3* strongly in the entire blastoderm margin (Fig. 3*B4*). Like-

DEVELOPMENTAL BIOLOGY

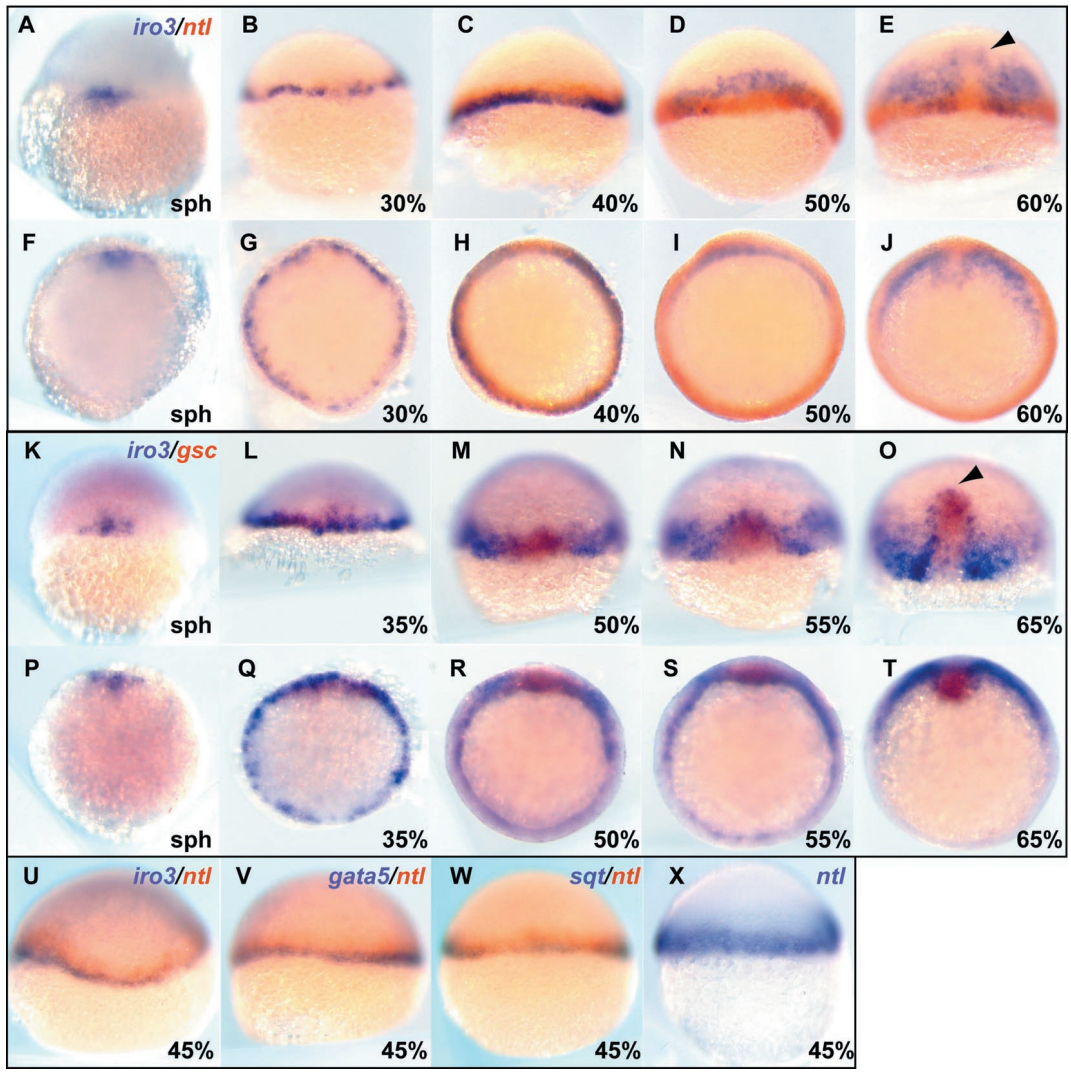

Fig. 2. Iro3 expression in the early mesendodermal layer. *Iro3* (purple) and the mesodermal marker *ntl* (red) (*A–J*), or the anterior axial marker *gsc* (red) (*K–T*), were visualized by double-staining *in situ* hybridization. At the sphere stage, *iro3* starts to be expressed at one side of the blastoderm margin (*A*), spreading across the margin subsequently (*B*). At 40% epibody, *ntl* expression extends slightly toward the animal pole, whereas *iro3* stays at the lower margin (*C*) but subsequently involutes as a deep layer (*D*, *I*, and *N*). At 60–65% epibody, axial mesendoderm differentially expresses *gsc* (anterior) and *ntl* (posterior). The *iro3* positive region extends to the most anterior end at the edges of the *gsc* expression domain but is excluded from the axial domain (*E* and *O*, arrowhead). Lower marginal expression of *iro3* is similar to the expression of *gata5* (*V*) and *sqt* (*W*), whereas *ntl* extends slightly further in the animal direction (*U* and *X*). *A–E*, *K–O*, and *U–X*, dorsal-lateral view; *F–J* and *P–T*, animal view.

wise, β-catenin mRNA injection induced ectopic *iro3* expression (Fig. 3 *G2* and *G4*). These results suggest that *iro3* expression during gastrulation is maintained dorsally by β-catenin-induced BMP antagonists. In *swr* mutants and in *noggin*-injected embryos, ventral deep cells expressed *iro3*, but this expression domain did not migrate toward the animal pole, unlike the natural, dorsal expression domain of *iro3* (Fig. 3 *B3* and *H2*, open and filled arrowheads, respectively). In contrast, the *iro3*-positive ventral region expanded toward the animal pole in β-catenin-injected embryos (Fig. 3*G4*). The same expansion was observed in embryos in which Noggin and the Wnt inhibitor Dkk1 were coexpressed (Fig. 3*H3*, open arrowhead); it is known that inhibition of BMP and Wnt signaling is required for anterior development in the gastrula (36).

***Iro3* Induces Organizer Markers in a Noncell Autonomous Manner.** To test the possible role of *iro3* in organizer formation, we injected *iro3* mRNA into two-to four-cell stage embryos and looked for the induction of organizer markers. *Iro3* was capable of inducing the organizer genes *lim1*, *axial* (*axl*), *chd*, *flh*, and *cyc* (Fig. 4 and data not shown). These genes were mostly induced just outside of the injected domain as visualized by β-gal staining, suggesting that *iro3* induces organizer gene expression in a noncell autonomous manner. In contrast to the genes mentioned above, *gsc*, a marker for the anterior-most axial mesoderm, was induced only weakly and inconsistently by *iro3*.

We sought to identify putative secreted molecules that might mediate *iro3* induction of organizer genes. However, *iro3* injection did not activate *sqt*, *cyc*, *dkk1*, *chd*, *follistatin*, or *noggin1* in the injected domain (not shown). We also examined the effect of *iro3* injection on the ventral markers *bmp2b* and *bmp4*. Embryos injected at the two-cell stage with *iro3* RNA showed decreased ventral expression of the *bmp* genes not only on the injected (red) but also the uninjected side (Fig. 4 *F* and *H*); the dorsal *bmp* domain was unaffected or occasionally expanded (arrowhead). As *iro3* seems to be expressed in the endoderm, we examined the endodermal genes *sox17*, *mixer*, and *gata5* in *iro3*-injected embryos but found none to be induced.

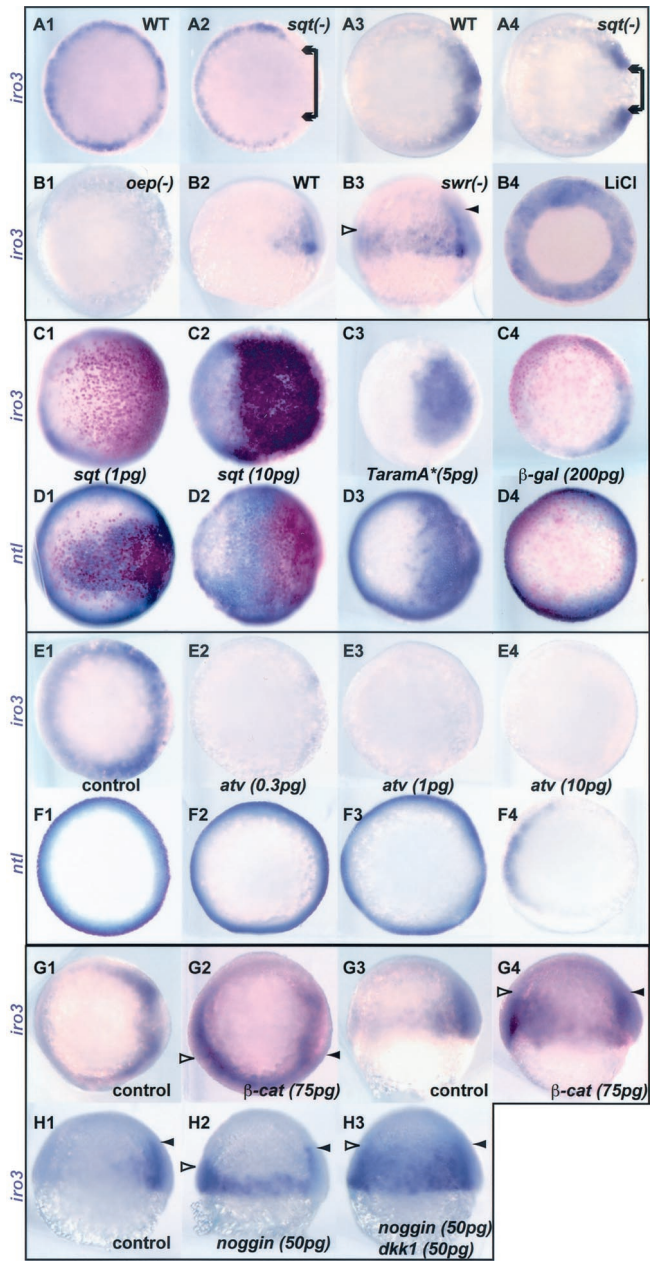

Fig. 3. *Iro3* expression is regulated by Nodal, β-catenin, and BMP antagonists. (*A* and *B*) Embryos mutant for *sqt* (*A2* and *A4*), *oep* (*B1*), and *swr* (*B3*), and LiCl-treated embryos (*B4*), were hybridized with *iro3*. In *sqt* embryos, there is a gap in *iro3* expression at the dorsal side (*A2* and *A4*, arrows). Zygotic *oep* mutant embryos do not express *iro3* during blastula and gastrula stages (*B1*). *Iro3* expression in the dorsal deep layer at early gastrula was expanded ventrally in *swr* embryos (*B3*) and LiCl-treated embryos (*B4*). (*C* and *D*) *Sqt* and *TaramA** mRNAs were injected into two- to four-cell stage embryos together with β-gal mRNA. Embryos were fixed at 45–55% epibody and stained for β-gal (red) and *iro3* (*C*) or *ntl* (*D*) (purple). *Sqt* induces *iro3* only at a high dose (*C2*), but *ntl* at all doses (*D1* and *D2*). (*E* and *F*) *Antivin* (*atv*) mRNA, encoding an antagonist of Nodal, was injected at different doses, and embryos at 45% epibody were stained for *iro3* (*E*) and *ntl* (*F*). Even a low dose of *atv* mRNA suppressed *iro3* (*E2*), whereas only a high dose suppressed *ntl* (*F4*). (*G* and *H*) Embryos were injected with RNAs encoding β-catenin and the BMP antagonist Noggin with or without the Wnt antagonist Dkk1, and were stained with *iro3* at 60% epibody. Note that in *swr* mutant and *noggin*-injected embryos, the *iro3* domain expanded ventrally but not toward the animal pole (*B3* and *H2*, open arrowhead), whereas in β-catenin or *noggin*+*dkk1* RNA-injected embryos, the ectopic *iro3* domain did expand toward the animal pole (*G4* and *H3*, open arrowhead). (*A*, *B1*, *B4*, *C–F*, *G1*, and *G2*) Animal view. (*B2*, *B3*, *G3*, *G4*, and *H*) Lateral view.

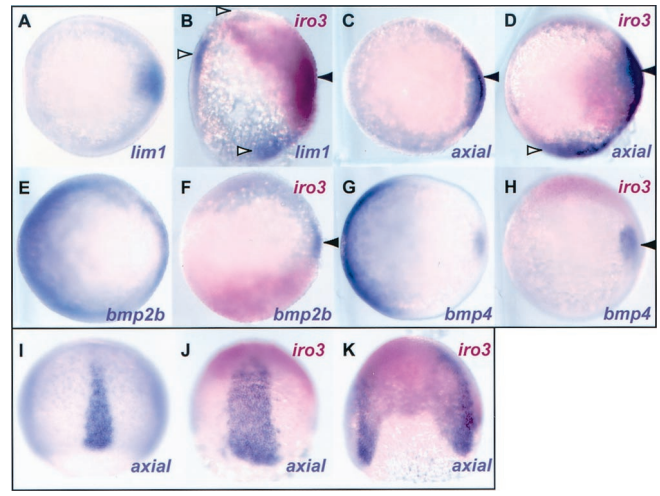

Fig. 4. *Iro3* induces dorsal and represses ventral markers in a noncell autonomous manner. *Iro3* mRNA (200 pg) was injected as indicated at the two- to four-cell stage together with β-gal mRNA, and embryos were fixed at the shield stage (*A–H*; animal view) or 90% epibody stage (*I–K*; dorsal view). Organizer markers, *lim1* (*A* and *B*) and *axial* (*C* and *D*), and ventral markers, *bmp2b* (*E* and *F*) and *bmp4* (*G* and *H*), were stained purple by *in situ* hybridization, and red staining identifies the injected region. *Lim1* and *axial* were activated in *iro3*-injected embryos outside the β-gal-positive region. The intrinsic expression domain (shield) and ectopic domain are indicated by filled and open arrowheads, respectively (*A–D*). Ventral expression of *bmp2b* and *bmp4* was suppressed in both the injected and uninjected side (*F* and *H*), but the dorsal expression domain of the *bmp2b* and *bmp4* was retained (arrowhead). At 90% epibody, the *axial*-stained notochord was expanded (*J*) or duplicated (*K*) in injected embryos.

When *iro3* mRNA was injected into eight- to 16-cell stage embryos, a low incidence (less than 10%) of secondary axis formation was observed. At least part of the reason for this low incidence may be that the injections could not be targeted to the future ventral domain. In addition, many embryos showed gastrulation defects and therefore could not be analyzed. Those secondary axes that did arise were incomplete, missing anterior structures. We also injected *iro3* mRNA into *Xenopus* embryos and observed efficient induction of incomplete secondary axes (65%, $n = 86$). Likewise, *Xenopus iro3* mRNA injected into *Xenopus* embryos induced secondary axes at similarly high efficiency. Thus, *iro3* is capable of inducing organizer activity in the ventral domain of different vertebrate embryos.

***VP-iro3* Inhibits Organizer Formation.** Artificial repressor (En-iro3) and activator (VP-iro3) forms of Iro3 were constructed, and the corresponding mRNAs were injected into one blastomere of two-cell zebrafish embryos (Fig. 5). *En-iro3* mRNA induced *axl* like wild-type *iro3* mRNA (Fig. 5 *B* and *C*). In contrast, *VP-iro3* mRNA injection decreased *axl* expression; repression of *axl* expression was seen in the injected side of the embryo, although both cells that were and that were not injected with tracer were affected (Fig. 5*D*). Coinjection of *iro3* and *VP-iro3* mRNAs induced *axl* like the wild type alone, showing that the interfering effect of *VP-iro3* could be rescued by coexpression of the wild-type form (Fig. 5*G*). These results indicate that *iro3* functions as a transcriptional repressor in organizer formation and that *VP-iro3* acts as a dominant negative or antimorphic form. The fact that Iro3, a repressor, activates expression of several genes suggests that this effect is indirect. This agrees with the noncell autonomous nature of the induction, which also implies involvement of a mediator.

Discussion

***Iro3* Marks a Specific Domain in the Early Mesendodermal Layer.** *Iro3* is expressed in the lower blastoderm margin at late blastula in a

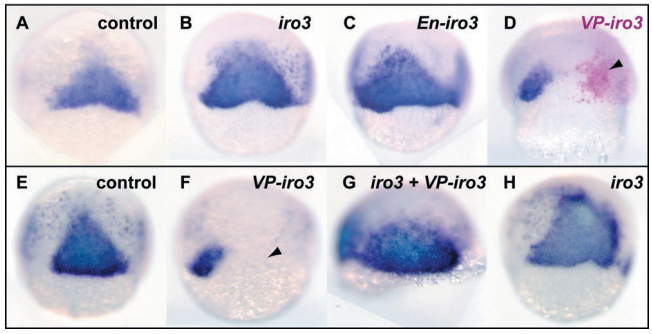

Fig. 5. Opposite effects of *iro3*/*en-iro3* and *VP-iro3* on *axial* induction. *Iro3* (*B* and *H*), *en-iro3* (*C*), or *VP-iro3* (*D* and *F*) mRNAs (200 pg) were injected at the two-cell stage into one blastomere. *Axial* was stained at 60% epibody. Whereas *iro3* and *en-iro3* injection induced *axial* strongly, *VP-iro3* injection suppressed *axial* around the injected area visualized by β-gal staining (*D*, arrowhead). When *iro3* and *VP-iro3* mRNAs (200 pg each) were coinjected, *axial* expanded (*G*), as by *iro3* single injection (*H*). All panels shown are dorsal views.

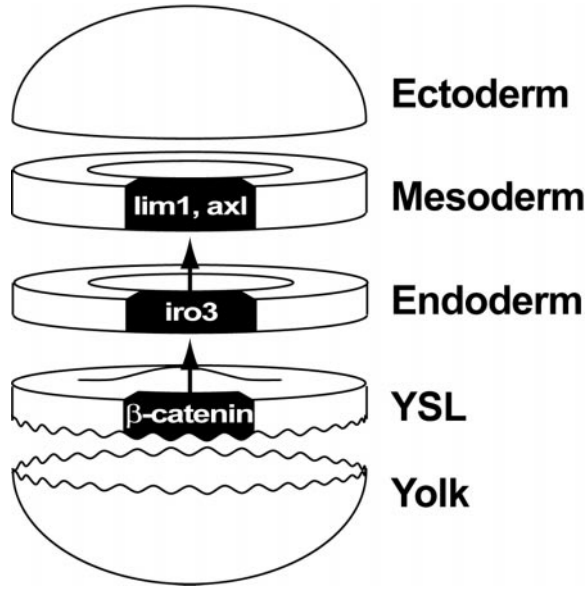

Fig. 6. A model for the position of *iro3* and the *iro3*-expressing dorsal endodermal domain in organizer patterning. In the dorsal YSL, the β-catenin signal is activated and *sqt* is expressed. The activation of *iro3* in the overlying endoderm depends on the function of the YSL. In turn, *iro3* has a role in inducing organizer genes in the overlying mesoderm, presumably through the mediation of an unknown secreted molecule. Each of the arrows implies multiple steps in molecular pathways. This model is similar to a model in *Xenopus* that distinguishes the Nieuwkoop center, late blastula organizer, and gastrula organizer. See text for additional details.

pattern similar to that of *gata5* (29) and different from *ntl*, which is expressed more widely, suggesting that most of the *iro3* expression domain gives rise to endodermal derivatives. During gastrulation, ventral *iro3* expression is lost while the dorsal *iro3* domain involutes, continuing to occupy a deep layer that migrates toward the animal pole. This behavior is consistent with lineage analysis, indicating that vegetal cells in the dorsal germ ring give rise to pharyngeal endoderm (37, 38).

***Iro3* Induction Requires a Nodal Signal.** *Iro3* was suppressed in the presumptive organizer region but not in ventro-lateral marginal cells in *sqt* mutants in a similar way as several other genes such as *lim1*, *ntl*, *gata5*, and *mixer* (29, 39) (data not shown). It appears that all mesendoderm specification is defective in the dorsal-most quadrant of *sqt* embryos. In contrast, *iro3* expression was unaffected in *cyc* embryos. The fact that the *oep* mutation affects *iro3* expression more strongly than *sqt* implies that *cyc* does play a role in *iro3* expression that is not apparent in *cyc* mutants because of some redundancy between the two Nodal factors (30, 31, 40, 41). In zygotic *oep* mutants where Nodal signaling is depressed (31, 42, 43), *iro3* expression was lost. Such mutants, however, retain some Nodal signal as a result of maternal *oep* mRNA. The total loss of *iro3* expression in zygotic *oep* embryos can be explained by the dependence of *iro3* on a strong Nodal signal (Fig. 3).

The BMP Pathway Regulates Dorsal Restriction of *iro3* Expression. Dorsal *iro3* expression was expanded ventrally by LiCl treatment, β-catenin, or *noggin* injection, and in *swr* mutants. These results suggest that ventral loss of *iro3* expression at the onset of gastrulation is caused by a BMP signal. *Iro3* expression was not affected in the *din* mutant where chordin activity is missing, presumably because of redundancy between BMP antagonists. In the mouse, *noggin* and *chordin* double knockout mutants show strong dorso-anterior defects, but single mutants do not (44, 45).

In *noggin*-injected and *swr* mutant embryos, *iro3* expression expanded ventrally but did not expand toward the animal pole, as the dorsal *iro3*-expressing domain does (Fig. 3 *B3* and *H2*). This suggests that suppression of the BMP signal is sufficient to activate *iro3* in the deep marginal cell layer but not to recruit these cells to anterior migration. In contrast, anterior expansion of the ectopic *iro3* domain was seen in β-catenin-injected embryos (Fig. 3*G4*), in agreement with the ability of β-catenin to induce complete secondary axes (2–4). A combination of BMP and Wnt antagonists likewise can induce complete axes (46), and coinjection of *noggin* and *dkk1* mRNAs led to ventral expression of *iro3* and expansion of the positive domain toward the animal pole (Fig. 3*H3*).

Noncell Autonomous Induction of Organizer Genes by *iro3*. *Iro3* mRNA injection induced ectopic expression of several organizer markers and suppressed ventral genes, both in a noncell autonomous manner. As dorsally restricted *iro3* expression is found adjacent to axial mesoderm forming the shield, an indirect effect of Iro3 on organizer formation may be expected. Such an indirect role also is suggested by the results indicating that Iro3 acts as a repressor, requiring at least one intermediate step in a pathway in which Iro3 elicits gene activation in the organizer. In the simplest model, Iro3 would repress the expression of a signaling factor that inhibits organizer formation. More complex models involving additional intermediate steps can be envisioned and remain to be explored.

Role of the *iro3*-Expressing Domain in Patterning the Mesendoderm. We suggest that *iro3*, activated by Nodal factors and restricted to the dorsal side by signals ultimately dependent on β-catenin, has an important role in patterning the mesendoderm in the early gastrula. The *iro3*-expressing domain may define a region with a distinct role in organizer formation in the early embryo. A multiple-organizer model, in which distinct regions act in temporal and spatial succession, has been proposed in *Xenopus* (1). The Nieuwkoop center is thought to induce the late blastula organizer in the vegetal half of the Spemann organizer; the blastula organizer region gives rise to head mesoderm, anterior notochord, anterior somites, and pharyngeal endoderm. The late blastula organizer, in turn, induces immediately above it the gastrula organizer, which develops into the notochord.

This model in *Xenopus* has some similarities in temporal and

spatial aspects to a model we suggest for zebrafish on the basis of our studies on *iro3* (Fig. 6). Here, the *iro3*-expressing domain corresponds to the *Xenopus* late blastula organizer and, like this structure, includes pharyngeal endoderm precursor cells. We suggest that the *iro3* domain is spatially and functionally interspersed between the YSL, which represents the Nieuwkoop center equivalent, and the gastrula organizer. In sum, we propose that the early expression domain of *iro3* marks a distinct region of the evolving organizer, and that Iro3 activity in this domain has an important role in organizer expansion and differentiation.

We thank Elizabeth Laver for assistance with zebrafish; N. Hukriede, A. Kawahara, and M. Tsang for discussion; M. Halpern and D. Stainier for comments on the manuscript; M. Mullins, A. Schier, and M. Halpern for mutant zebrafish lines; B. Thisse for *antivin* and *noggin1*; R. Patient for *gata5*; F. Rosa for *TaramA**; N. Ueno for *bmp* cDNAs; and M. Hibi for mouse *noggin* and *dkk1*.

1. Gerhart, J. C., Stewart, R. & Doniach, T. (1991) in *Gastrulation: Movement, Patterns, and Molecules*, eds. Keller, R., Clark, W., Jr., & Griffin, F. (Plenum, New York), pp. 57–77.
2. Funayama, N., Fagotto, F., McCrea, P. & Gumbiner, B. M. (1995) *J. Cell Biol.* **128,** 959–968.
3. Heasman, J., Crawford, A., Goldstone, K., Garner-Hamrick, P., Gumbiner, B., McCrea, P., Kintner, C., Noro, C. Y. & Wylie, C. (1994) *Cell* **79,** 791–803.
4. Kelly, G. M., Erezyilmaz, D. F. & Moon, R. T. (1995) *Mech. Dev.* **53,** 261–273.
5. Long, W. L. (1983) *J. Exp. Zool.* **228,** 91–97.
6. Mizuno, T., Yamanaka, M., Wakahara, A., Kuroiwa, A. & Takeda, H. (1996) *Nature (London)* **383,** 131–132.
7. Schneider, S., Steinbeisser, H., Warga, R. M. & Hausen, P. (1996) *Mech. Dev.* **57,** 191–198.
8. Fekany, K., Yamanaka, Y., Leung, T., Sirotkin, H. I., Topczewski, J., Gates, M. A., Hibi, M., Renucci, A., Stemple, D., Radbill, A., *et al.* (1999) *Development (Cambridge, U.K.)* **126,** 1427–1438.
9. Koos, D. S. & Ho, R. K. (1998) *Curr. Biol.* **8,** 1199–1206.
10. Yamanaka, Y., Mizuno, T., Sasai, Y., Kishi, M., Takeda, H., Kim, C. H., Hibi, M. & Hirano, T. (1998) *Genes Dev.* **12,** 2345–2353.
11. Kodjabachian, L., Dawid, I. B. & Toyama, R. (1999) *Dev. Biol.* **213,** 231–245.
12. Bouwmeester, T. & Leyns, L. (1997) *BioEssays* **19,** 855–863.
13. Gomez-Skarmeta, J. L., del Corral, R. D., de la Calle-Mustienes, E., Ferre-Marco, D. & Modolell, J. (1996) *Cell* **85,** 95–105.
14. McNeill, H., Yang, C. H., Brodsky, M., Ungos, J. & Simon, M. A. (1997) *Genes Dev.* **11,** 1073–1082.
15. Cavodeassi, F., Diez Del Corral, R., Campuzano, S. & Dominguez, M. (1999) *Development (Cambridge, U.K.)* **126,** 4933–4942.
16. Cavodeassi, F., Modolell, J. & Campuzano, S. (2000) *Development (Cambridge, U.K.)* **127,** 1921–1929.
17. Diez del Corral, R., Aroca, P., Gomez-Skarmeta, J. L., Cavodeassi, F. & Modolell, J. (1999) *Genes Dev.* **13,** 1754–1761.
18. Grillenzoni, N., van Helden, J., Dambly-Chaudiere, C. & Ghysen, A. (1998) *Development (Cambridge, U.K.)* **125,** 3563–3569.
19. Leyns, L., Gomez-Skarmeta, J. L. & Dambly-Chaudiere, C. (1996) *Mech. Dev.* **59,** 63–72.
20. Bellefroid, E. J., Kobbe, A., Gruss, P., Pieler, T., Gurdon, J. B. & Papalopulu, N. (1998) *EMBO J.* **17,** 191–203.
21. Gomez-Skarmeta, J. L., Glavic, A., de la Calle-Mustienes, E., Modolell, J. & Mayor, R. (1998) *EMBO J.* **17,** 181–190.
22. Bao, Z. Z., Bruneau, B. G., Seidman, J. G., Seidman, C. E. & Cepko, C. L. (1999) *Science* **283,** 1161–1164.
23. Tan, J. T., Korzh, V. & Gong, Z. (1999) *Mech. Dev.* **87,** 165–168.
24. Hukriede, N. A., Joly, L., Tsang, M., Miles, J., Tellis, P., Epstein, J. A., Barbazuk, W. B., Li, F. N., Paw, B., Postlethwait, J. H., *et al.* (1999) *Proc. Natl. Acad. Sci. USA* **96,** 9745–9750.
25. Kessler, D. S. (1997) *Proc. Natl. Acad. Sci. USA* **94,** 13017–13022.
26. Rebagliati, M. R., Toyama, R., Fricke, C., Haffter, P. & Dawid, I. B. (1998) *Dev. Biol.* **199,** 261–272.
27. Renucci, A., Lemarchandel, V. & Rosa, F. (1996) *Development (Cambridge, U.K.)* **122,** 3735–3743.
28. Toyama, R., Curtiss, P. E., Otani, H., Kimura, M., Dawid, I. B. & Taira, M. (1995) *Dev. Biol.* **170,** 583–593.
29. Rodaway, A., Takeda, H., Koshida, S., Broadbent, J., Price, B., Smith, J. C., Patient, R. & Holder, N. (1999) *Development (Cambridge, U.K.)* **126,** 3067–3078.
30. Feldman, B., Gates, M. A., Egan, E. S., Dougan, S. T., Rennebeck, G., Sirotkin, H. I., Schier, A. F. & Talbot, W. S. (1998) *Nature (London)* **395,** 181–185.
31. Gritsman, K., Zhang, J., Cheng, S., Heckscher, E., Talbot, W. S. & Schier, A. F. (1999) *Cell* **97,** 121–132.
32. Born, J., Geithe, H.-P., Tiedemann, H., Tiedemann, H. & Kocher-Becker, U. (1972) *Z. Phys. Chem. (Leipzig)* **353,** 1075–1084.
33. Weber, H., Symes, C. E., Walmsley, M. E., Rodaway, A. R. & Patient, R. K. (2000) *Development (Cambridge, U.K.)* **127,** 4345–4360.
34. Yasuo, H. & Lemaire, P. (1999) *Curr. Biol.* **9,** 869–879.
35. Kishimoto, Y., Lee, K. H., Zon, L., Hammerschmidt, M. & Schulte-Merker, S. (1997) *Development (Cambridge, U.K.)* **124,** 4457–4466.
36. Kimelman, D. & Griffin, K. J. P. (2000) *Curr. Opin. Genet. Dev.* **10,** 350–356.
37. Kimmel, C. B., Warga, R. M. & Schilling, T. F. (1990) *Development (Cambridge, U.K.)* **108,** 581–594.
38. Warga, R. M. & Nusslein-Volhard, C. (1999) *Development (Cambridge, U.K.)* **126,** 827–838.
39. Alexander, J. & Stainier, D. Y. (1999) *Curr. Biol.* **9,** 1147–1157.
40. Sampath, K., Rubinstein, A. L., Cheng, A. M., Liang, J. O., Fekany, K., Solnica-Krezel, L., Korzh, V., Halpern, M. E. & Wright, C. V. (1998) *Nature (London)* **395,** 185–189.
41. Rebagliati, M. R., Toyama, R., Haffter, P. & Dawid, I. B. (1998) *Proc. Natl. Acad. Sci. USA* **95,** 9932–9937.
42. Schier, A. F., Neuhauss, S. C., Helde, K. A., Talbot, W. S. & Driever, W. (1997) *Development (Cambridge, U.K.)* **124,** 327–342.
43. Hammerschmidt, M., Pelegri, F., Mullins, M. C., Kane, D. A., Brand, M., van Eeden, F. J., Furutani-Seiki, M., Granato, M., Haffter, P., Heisenberg, C. P., *et al.* (1996) *Development (Cambridge, U.K.)* **123,** 143–151.
44. McMahon, J. A., Takada, S., Zimmerman, L. B., Fan, C. M., Harland, R. M. & McMahon, A. P. (1998) *Genes Dev.* **12,** 1438–1452.
45. Bachiller, D., Klingensmith, J., Kemp, C., Belo, J. A., Anderson, R. M., May, S. R., McMahon, J. A., McMahon, A. P., Harland, R. M., Rossant, J. & De Robertis, E. M. (2000) *Nature (London)* **403,** 658–661.
46. Glinka, A., Wu, W., Onichtchouk, D., Blumenstock, C. & Niehrs, C. (1997) *Nature (London)* **389,** 517–519.